Journal of Hazardous Materials 169 (2009) 635–642

Contents lists available at ScienceDirect

Journal of Hazardous Materials

journal homepage: www.elsevier.com/locate/jhazmat

Effect of Al_2O_3 mole fraction and cooling method on vitrification of an artificial hazardous material. Part 2: Encapsulation of metals and resistance to acid

Yi-Ming Kuo [a,*], Chih-Ta Wang [a], Jian-Wen Wang [a], Kuo-Lin Huang [b]

[a] Department of Safety Health and Environmental Engineering, Chung Hwa University of Medical Technology, Tainan County, 71703, Taiwan, ROC
[b] Department of Environmental Engineering and Science, National Pingtung University of Science and Technology, Ping Tung 91201, Taiwan, ROC

ARTICLE INFO

Article history:
Received 21 November 2008
Received in revised form 30 March 2009
Accepted 30 March 2009
Available online 9 April 2009

Keywords:
Al ion
Encapsulation
Vitrification
Slag
Acid immersion

ABSTRACT

This study investigated the encapsulation of metals in vitrified slags using a sequential extraction procedure and how Al ions and slag structure affected the encapsulation of heavy metals. It is found that the substitution of Al ions for Si ions weakened the encapsulation of the glass matrix due to the relatively weaker single bond strength of Al–O. In addition, the substitution also governed the phase distribution of metals that tended to stay slags. In comparison to air cooled slags, water quenched slags were more amorphous and offered relatively better encapsulation of metals. These findings were also supported by the SEM observation and XRD analysis. Although Al_2O_3 may connect the non-bridging oxygen and polymerize the slag structure, the excess addition of Al_2O_3 reduced the metal encapsulation and acid resistance of slags.

1. Introduction

For the final disposal of hazardous waste, the immobilization or stabilization of toxic metals is important because of environmental concerns. There are several technologies available for the treatment of hazardous materials, such as solidification/stabilization, chemical leaching, sintering, and vitrification [1–3]. Among current technologies, solidification with cement is the most common way for immobilizing hazardous materials such as fly ash, sludge, or other toxic wastes [4,5]. This technology is economically favorable, but it inevitably increases the volume and weight of wastes. In addition, the solidified wastes are commonly dumped into landfill sites, and this operation is at the risk of secondary pollution due to metal leaching after a long period of time [6].

Although vitrification is an energy-consuming technology with high equipment cost, it is still widely used to treat hazardous material due to its good ability to reduce the mobility of hazardous metals, destroy organic toxics and recover metals [7–9]. The vitrification products include slag, ingot and secondary fly ash, with the latter two rich in valuable metals and commonly sent to smelters for metal recovery [10], while the slag is often reused as a building material or an additive for cement [11,12]. Therefore, the immobilization of metals in slags is especially important for public health.

Part 1 of this study investigated how Al ions and the cooling method dominated the formation of crystalline phase and glassy amorphous structure of slag. In addition, the metal leaching behavior was also evaluated by the toxic characteristic leaching procedure (TCLP) which simulates the scouring of acid rain. However, the TCLP results only show temporary metal leaching concentrations, not the metal encapsulation in slags. Therefore, the encapsulation of hazardous metals in the vitrified slags was evaluated by a sequential extraction procedure in this study. In addition, the correlation between the Al ions and encapsulation of metals was also discussed.

2. Experimental

2.1. Sample preparation and vitrification process

Pure powdery Al_2O_3, CaO, and SiO_2 served as the glassy encapsulation phases and Cr, Cu, Mn, Ni, and Pb were used as the targeted hazardous metals for investigating the correlation between the immobilization of hazardous metals and a glassy matrix during vitrification. The hazardous metal species were added in the forms of nitrate, including $Cr(NO_3)_3{\cdot}9H_2O$, $Cu(NO_3)_2{\cdot}3H_2O$, $Mn(NO_3)_2{\cdot}4H_2O$, $Ni(NO_3)_2{\cdot}6H_2O$, and $Pb(NO_3)_2$, with an identical concentration of 1000 mg/kg (as metal ions). For the glass matrix, the mass ratio of CaO to SiO_2, used as a control parameter, was kept at 2/3, and the mole fraction of Al_2O_3 in the glassy matrix served as an operation parameter. The compositions of the ternary glass matrix in mol% in the specimens are shown in Table 1.

* Corresponding author. Tel.: +886 6 2674567x854; fax: +886 6 2675049.
E-mail address: yiming@mail.hwai.edu.tw (Y.-M. Kuo).

0304-3894/$ – see front matter © 2009 Elsevier B.V. All rights reserved.
doi:10.1016/j.jhazmat.2009.03.151

Table 1
Glass matrix compositions (in mol%) of original specimens.

Specimen	Al_2O_3 (as Al ions)	CaO (as Ca ions)	SiO_2 (as Si ions)
A-0 and W-0	0.0	41.7	58.3
A-1 and W-1	5.7	39.3	55.0
A-2 and W-2	11.3	37.0	51.8
A-3 and W-3	16.8	34.7	48.5
A-4 and W-4	22.2	32.4	45.4
A-5 and W-5	27.6	30.2	42.2
A-6 and W-6	32.9	28.0	39.1

Powdery samples held in graphite crucibles were vitrified using an electrical melting furnace. The specimens were heated from 50 to 1100 °C at 6 °C/min and from 1100 to 1400 °C at 4 °C/min, respectively, using with $MoSi_2$ alloy heating rods. There are two different cooling methods. The samples cooled by air without forced convection were labeled with the prefixes of A and those cooled by water quenching were labeled with the prefixes of W (Table 1).

2.2. Sequential extraction for evaluating metal mobility of slags

The vitrified slags were dried at 105 °C for 3 h, weighed, pulverized and grinded to a size which could pass a mesh 200 sieve (smaller than 74 μm). To assess the mobility of metals, a sequential extraction protocol (Steps I–V) with five leaching steps was adopted [13]. According to the extraction scheme, the metals were divided into five phases using a solution with a successively decreasing pH in each step.

2.2.1. Carbonate phase

Each sample (0.5 g) was mixed with 20 mL, 0.1 M of acetic acid/sodium acetate (CH_3COOH/CH_3COONa) and shaken for 18 h. The samples were centrifuged with 1000 rpm for 5 min and filtrated using a cellulose ester filter with a pore size of 0.8 μm. The residues were then extracted by the following steps and the leaching solutions were analyzed by atomic absorption spectrometry (AAS, Sens AA, GBC).

2.2.2. Easily reducible phase

The mixture of residual samples from Step I and a 20 mL, 0.1 M hydroxylammonium chloride ($NH_2OH{\cdot}HCl$) solution were mixed and shaken for 18 h. The sample was then treated using the centrifugation/filtration in Step I and analysis in Steps II–IV.

2.2.3. Moderately reducible phase

The residue was extracted with 20 mL, 0.1 M of oxalic acid/ammonium oxalate [$H_2C_2O_4/(NH_4)_2C_2O_4$] solution for 18 h.

2.2.4. Sulfide phase

The residues from Step III were added into 10 mL hydrogen peroxide (30%). After the hydrogen peroxide solution was completely decomposed, a 10 mL, 0.1 M ammonium acetate (CH_3COONH_4) was added into the mixture and was shaken for 18 h.

2.2.5. Residual phase

The residue was digested with mixed acid (5 mL nitric acid [HNO_3] + 10 mL perchloric acid [$HClO_4$] + 1 mL fluoroboric acid [HBF_4]) in Teflon vessels by a microwave digester. The heating program for the digesting process was 25–180 °C at 10 °C/min, held isothermally for 15 min, and then cooled to room temperature. The digests were diluted to 25 mL with deionized water, filtrated with a cellulose ester filter with the pore size of 0.8 μm, and analyzed by atomic absorption spectroscopy (AAS, Sens AA, GBC).

In this study, three representative phases, namely the easily mobile phase (carbonate phase), moderately mobile phase (the summation of moderately reducible phase and sulfide phase), and stable phase (residual phase), were used to evaluate the metal encapsulation behavior of samples. The fractions of the three phases refer to the metals leached out during the period of slag structure decomposition that may be no decomposition, initial decomposition, or thorough decomposition [14].

2.3. Acid immersion test

To evaluate the acid resistance of slags, 1 g of each powdery specimen was immersed in a 100 mL, 3% of hydrochloric acid (HCl) solution for 7 days. Then, it was filtrated and analyzed as the procedures above to determine the concentrations of metals leached in the acid solution. The acid-immersed solid samples were washed with deionic water, dried, and examined by a scanning electron microscope for surface analysis and an X-ray diffraction (XRD) diffractometer for crystalline phase identification. The variation of crystalline phases and microstructures of slags before and after

Table 2
Content and PMR data of hazardous metals in slags.

Targeted metal	A-0				W-0			
	Range (mg/kg)	Average (mg/kg)	RSD (%)	PMR	Range (mg/kg)	Average (mg/kg)	RSD (%)	PMR
Cr	1220–1260	1240	1.90	1.23	969–1070	1015	5.12	1.23
Cu	767–902	855	8.91	0.847	451–563	517	11.4	0.512
Mn	1410–1530	1452	4.50	1.44	1170–1366	1269	7.71	1.26
Ni	1020–1250	1130	9.87	1.12	726–854	809	8.88	0.801
Pb	176–181	178	3.30	0.176	193–200	197	2.80	0.199

RSD: relative standard deviation = (standard deviation/average) × 100%.

Table 3
Variation of slag structure versus mole fraction of Al ions.

	Stage I	Stage II		Stage III		Stage IV	
Specimen	A-0	A-1	A-2	A-3	A-4	A-5	A-6
Al mol%	0	>0–15		15–25		>25	
AVF (%)	25.7	40–50		>90		78.6	46.5
NBO/T of the glass matrix	1.43	1.22	0.99	0.74	0.45	0.12	0
Predominate crystalline phase	$CaSiO_3$	$CaSiO_3$		None		$CaAl_2Si_2O_8$	
Category of crystalline phase	Inosilicate	Inosilicate		–		Tectosilicate	
Role of Al ions	–	Intermediate		Intermediate and network former		Network former	

NBO/T: ratio of non-bridging oxygens to tetrahedrally coordinated cation.

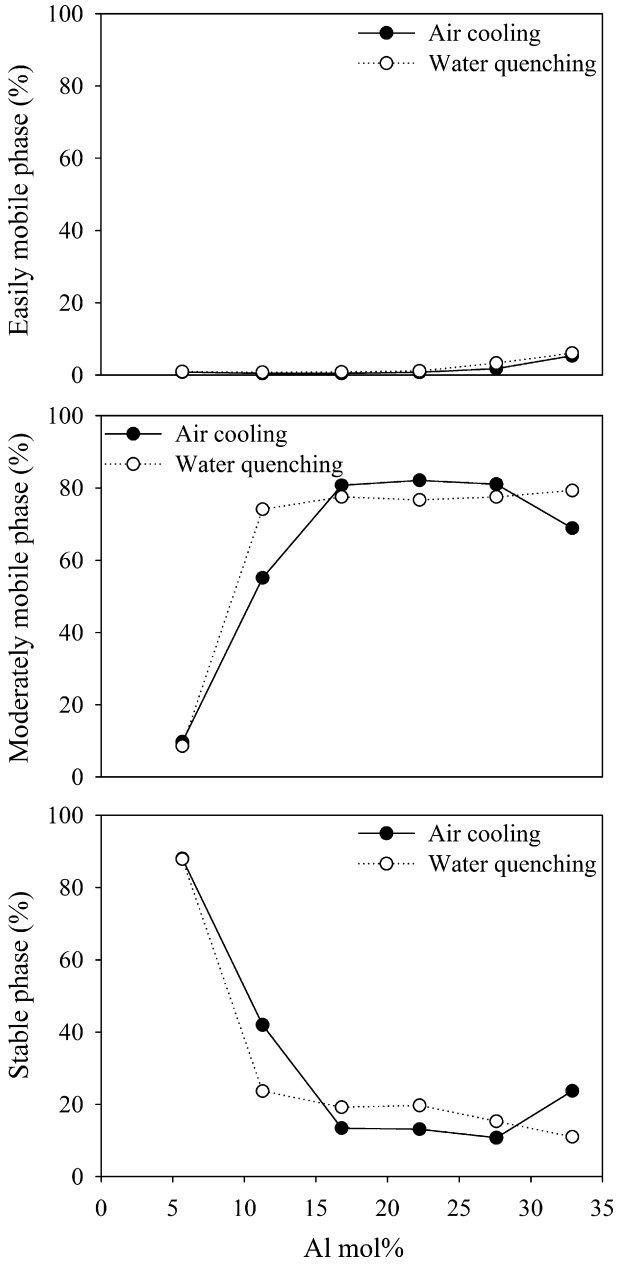

Fig. 1. Encapsulation behavior of Al in slags.

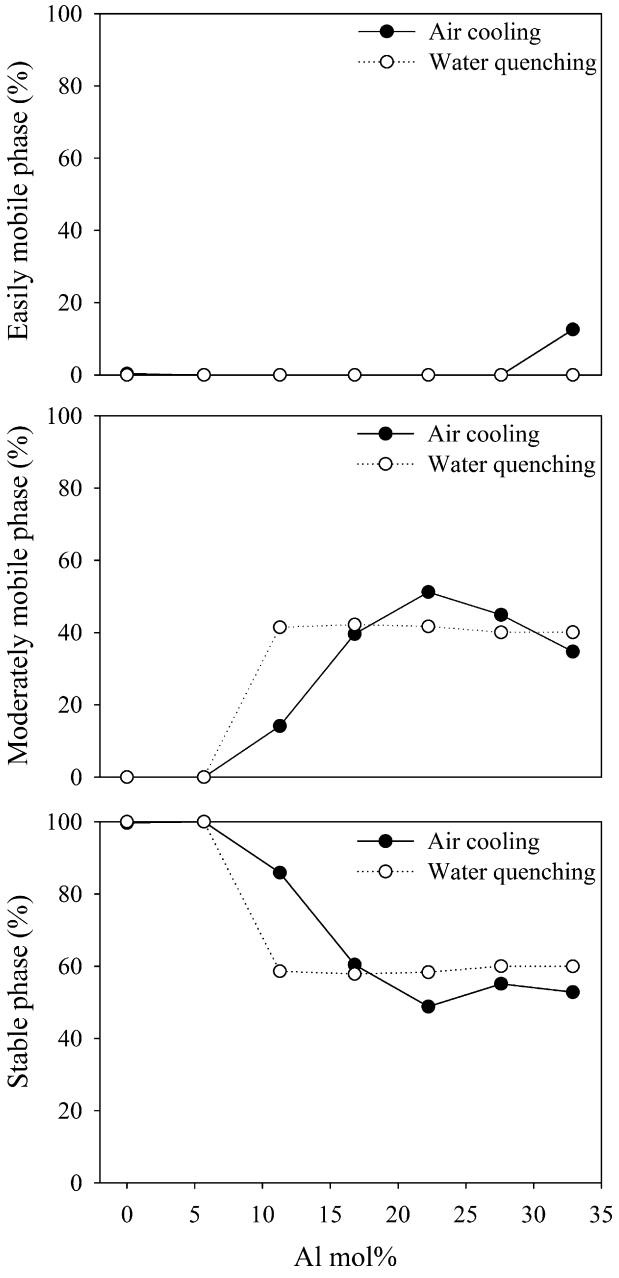

Fig. 2. Encapsulation behavior of Cr in slags.

acid immersion were used to evaluate the acid resistance of slag structure.

2.4. Evaluation of crystalline characteristics and microstructures

The XRD analysis was utilized to determine the variation of crystalline phases in air cooled slags with acid immersion. Acid leached samples were ground into fine powders with particle sizes <74 μm and analyzed using a powder diffractometer (Geigerflex 3063) with Ni-filtered CuK_α radiation. A range of 2θ angles from 20° to 60° was adopted to scan specimens using a detector with a step size of 0.01° and a dwell time of 0.15 s/step. The information of crystalline phases is provided in our another paper (Part 1). The volume fractions of crystalline phase in acid-immersed slags were measured using a semi-quantitative XRD technique with internal standard addition [15,16]. The detail analysis procedures were also given in Part 1.

Specimens pulverized to <74 μm particles were stuck on a metallic plate, coated with a gold film and scanned by the scanning electron microscopy—energy dispersive spectroscopy (SEM–EDS) (Jeol JXA-840) to qualitatively examine the microstructure of the slags.

3. Results and discussion

3.1. Compositions and crystalline characteristics of slags

Tables 2 and 3 taken from Part 1 show the compositions and crystalline characteristics of slags to serve as a reference to evaluate the encapsulation behaviors of heavy metals and the resistance to acid. The PMR (percent mass retained) = (mass retained in slag/mass in original specimen) × 100% of metals indicates that most Cr, Cu, Mn, and Ni remained in the slag, but most Pb was vaporized. With the variation of Al mol%, the four stages of slag crystalline structure variation defined in Part 1 are used to describe the role of Al ions during vitrification. With a successive increase in Al mol%,

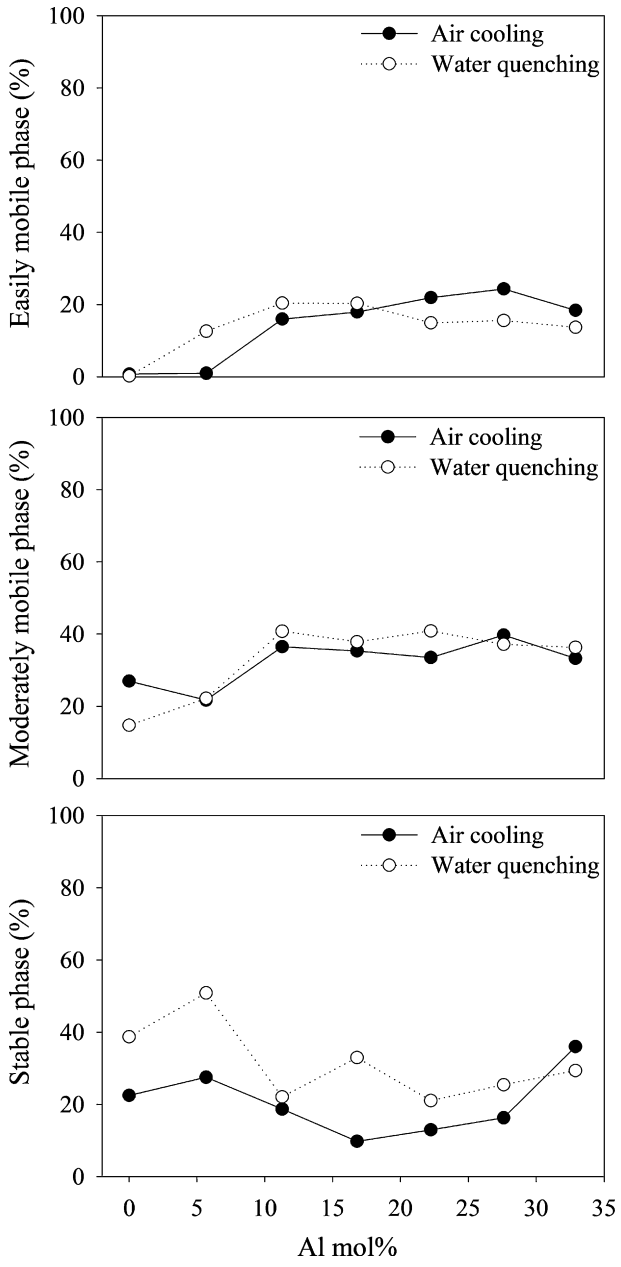

Fig. 3. Encapsulation behavior of Cu in slags.

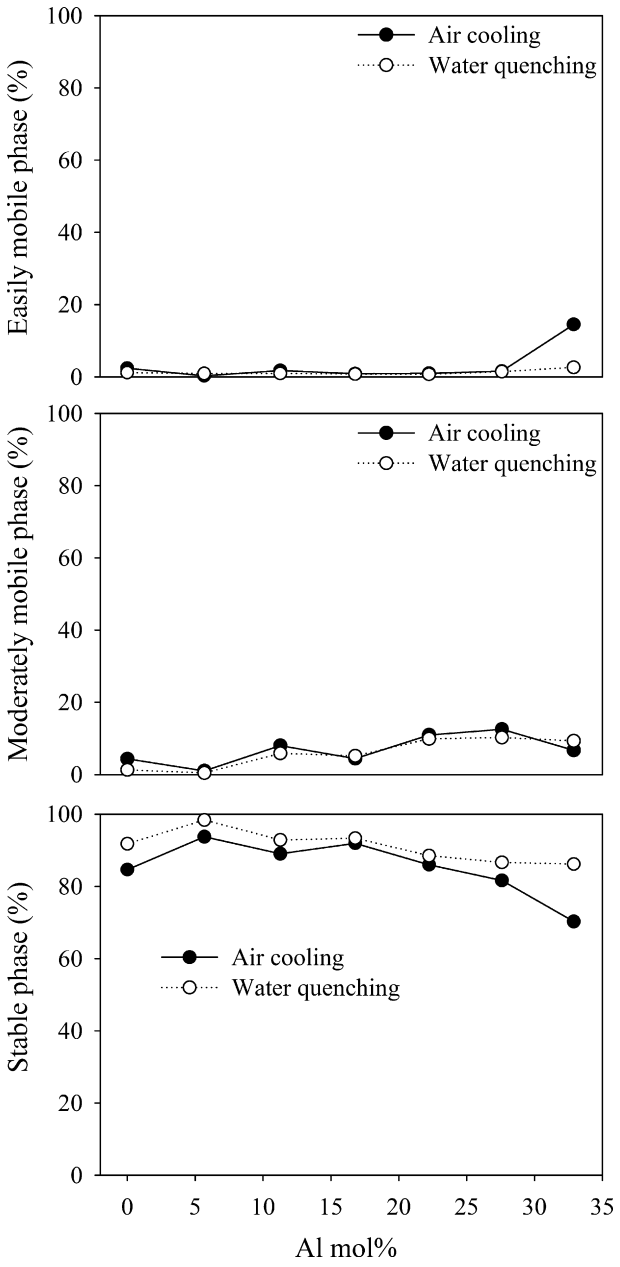

Fig. 4. Encapsulation behavior of Mn in slags.

Al ions acted as an intermediate, both an intermediate and a network former, and a network former in order. The Al ions caused the increase of amorphous volume fraction as Al mol% increased initially, but the amorphous volume fraction decreased when the Al mol% was higher than 25%. This finding indicates that Al ions connected with the silicate chain and polymerized the slag structure (see the explanation in Part 1).

3.2. Encapsulation of metals in slags

Figs. 1–6 show the mobile phase distribution of metals in slags. For Al, the availability of the easy mobile phase was all smaller than 5% and was slightly elevated in A-6 and W-6. At first, about 90% of Al ions existed as the stable phase, with an Al mol% of 5%. With higher Al mol%, the availability of the moderately mobile phase greatly increased to about 75% and was kept approximately constant. After vitrification, Al ions existed as the stable phase with a very low Al mol%, and it acted as an intermediate in the glass matrix and linked one SiO_4 tetrahedron chain to another. With a higher Al mol%, the Al ions started to replace Si ions and to be incorporated into the glass matrix. At this situation, the Al ions acted as both an intermediate and a network former and were transformed into moderately mobile phase.

For vitrification, Si and Al ions are the most important constituents in the glass networks of slags, and Al ions will replace Si ions to result in polymerization of the structure in an Al-rich environment. The substitution of ions and polymerization of the structure greatly affect the chemical stability of slags. A previous study reported that Al and Si in glass networks predominately existed as the moderately mobile and stable phases, respectively [17]. At the viewpoint of glass chemistry, the single bond strengths of Al–O and Si–O acting as a glass former are on average 90 and 106 kcal/g atom, respectively [18]. Therefore, it is concluded that the substitution of Al for Si may reduce the encapsulation effect of slag due to the weaker single bond strengths of Al–O and this can

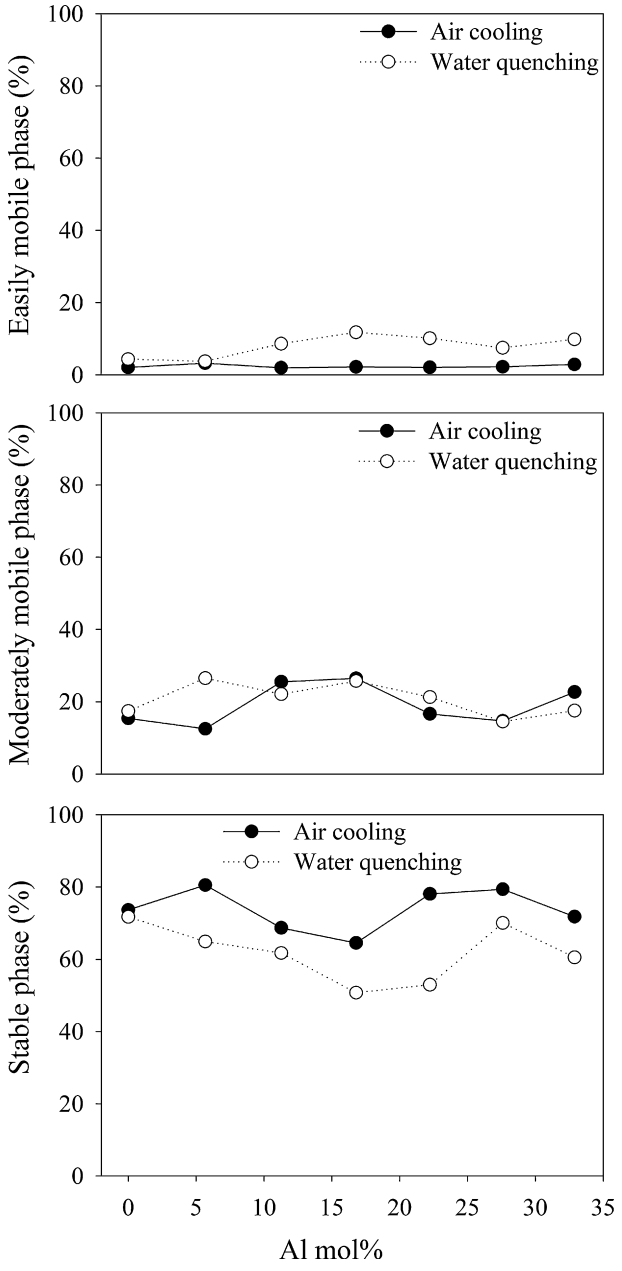

Fig. 5. Encapsulation behavior of Ni in slags.

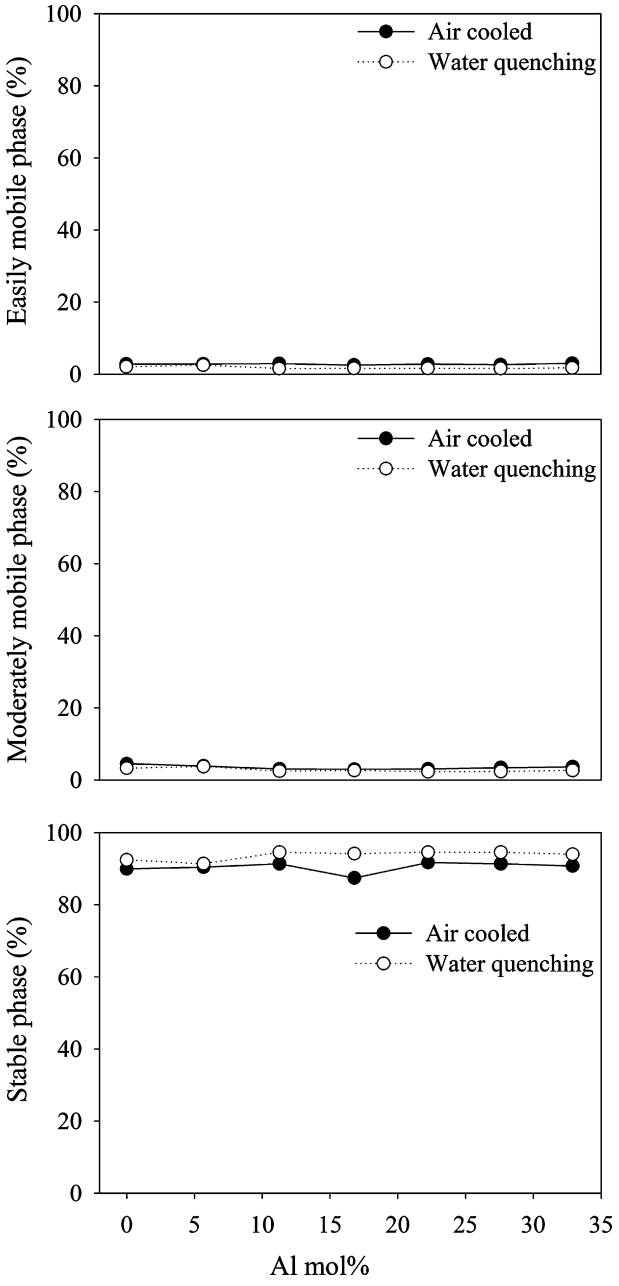

Fig. 6. Encapsulation behavior of Pb in slags.

explain why most of the stable phase of Al transformed into the moderately mobile phase when the Al mol% increased.

For Cr, the fraction of the easily mobile phase in slags was about zero, indicating that Cr was not leached when the slag structure was not decomposed. The availability of the moderately mobile phase increased to about 40% with Al mol% more than 10%, resulting in the decrease of the fraction of stable phase. In comparison to the mobile phase distribution, the trend of Cr versus Al mol% was similar to that of Al. It was reported that no ingot was generated in the vitrification of Cr electroplating sludge [19], implying that most of the Cr stayed in the slag and thus the leaching behavior of Cr was highly related to the slag structure. The leaching of moderately mobile Al resulted in the initial decomposition of the slag structure, and also caused Cr present as the moderately mobile phase, to be leached out.

The fraction of Cu in the easily mobile phase was <10% at Al mol% <10% while it was ~20% when Al mol% was >10%. A similar trend was seen in the moderately mobile phase but the fraction was slightly higher. The fraction of stable phase ranged from 10% to 40% and from 20% to 50% in air cooled and water quenched slags, respectively. Overall, water quenched slags offered better encapsulation of Cu. For Mn, about 80–90% of its mass was encapsulated in the stable phase, and the percentage remained constant with the variation of Al mol%. For Ni, the mobile phase distribution had no direct relationship with Al mol%, and about 80% of the Ni was encapsulated in the stable phase. The phase distribution pattern of Pb was similar to that of Ni, and the fraction of the stable phase was even higher, up to 90%.

A previous study indicated that most of the Cu, Mn, and Ni was retained in ingot and Pb was evaporated into the flue gas [9]. In this study, the encapsulation of Mn, Ni, and Pb was not significantly associated to the slag structure and Al mol%. Conversely, the phase distributions of the Al and Cr that predominately remained in slags had a noteworthy connection with Al mol%. During vitrification, the graphite may serve as a reductant to reduce Cu, Mn, and Ni,

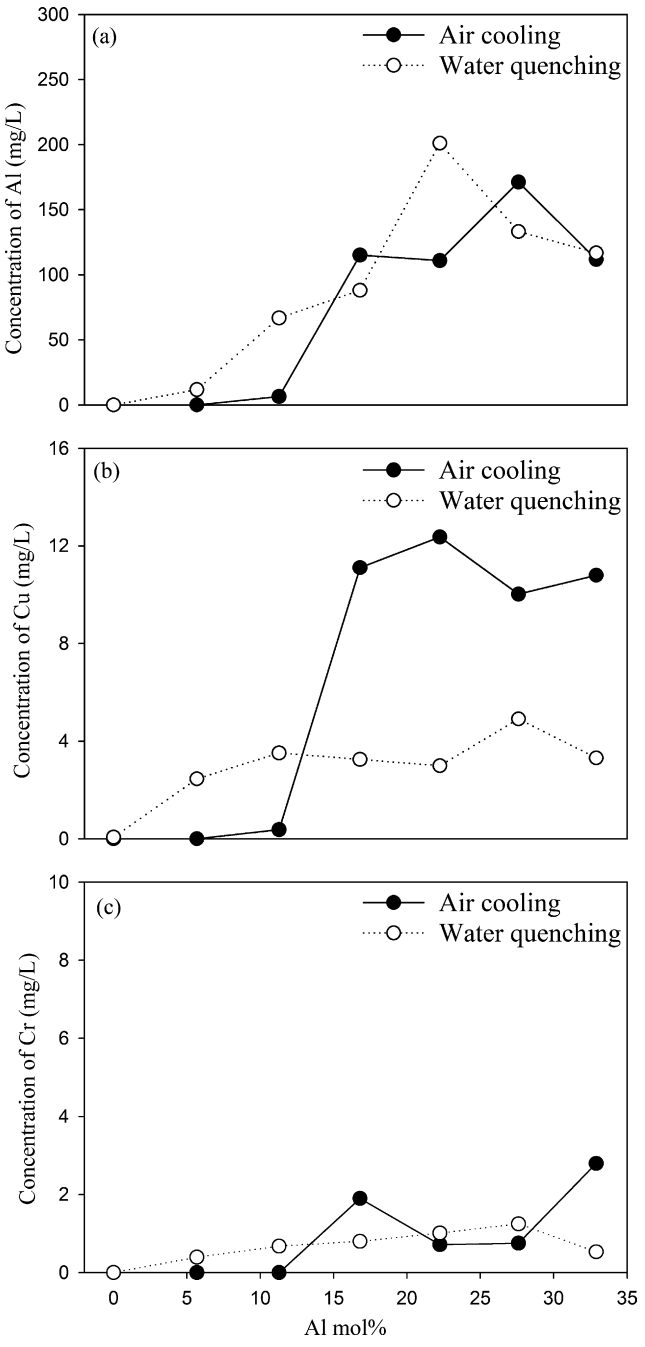

Fig. 7. Concentrations of (a) Al, (b) Cu, and (c) Cr in acid-leaching solutions.

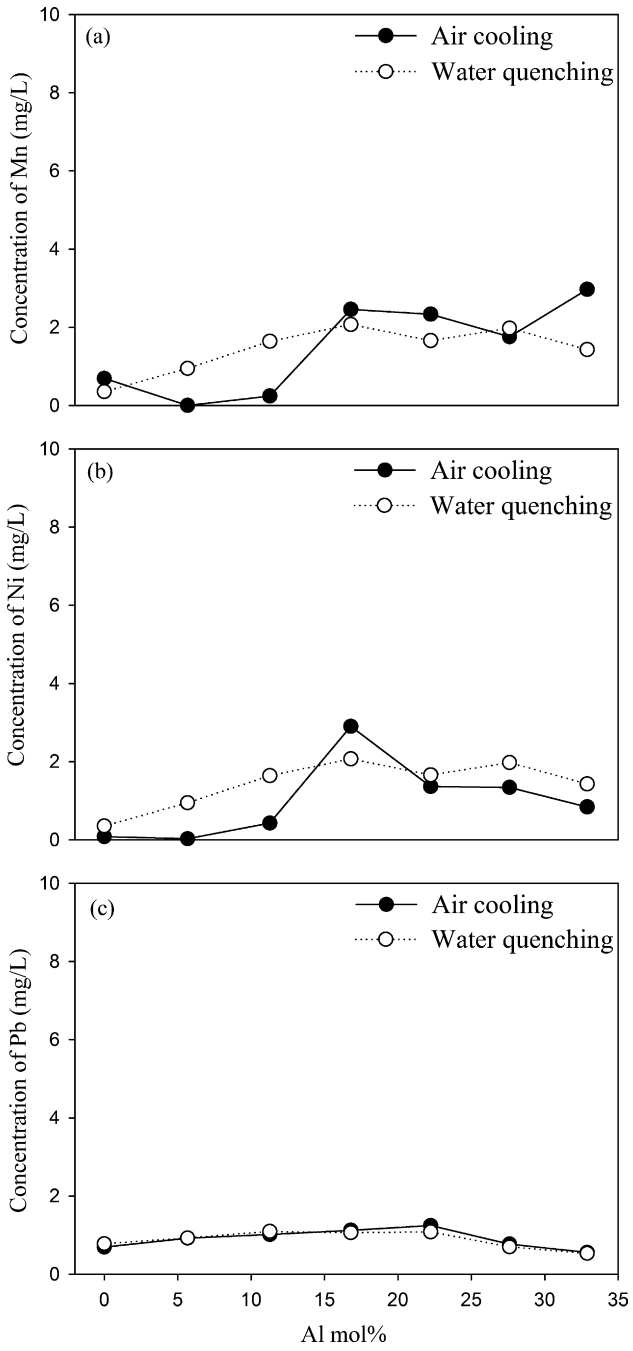

Fig. 8. Concentrations of (a) Mn, (b) Ni, and (c) Pb in acid-leaching solutions.

but it cannot reduce Al and Cr. Thus, Al and Cr, in oxidative forms, were incorporated with the glassy matrix and the encapsulation was highly connected the slag structure. In contrast, Cu, Mn and Ni, in elemental forms, were isolated from the glassy matrix, and no correlation between the encapsulation and the slag structure was found. These results clearly indicate that the encapsulation of metals that tended to move to ingot or flue gas was not significantly related with the slag structure or the Al mol%. However, for the metals tending to remain in slags, the form of metals and the incorporation with glassy matrix might govern the encapsulation of them.

3.3. Acid-leaching behavior of metals

Figs. 7 and 8 illustrate the leaching concentration of metals in the acid immersing solution. The leaching concentration of Al increased significantly to higher than 100 mg/L with Al mol% >15%, in air cooled or water quenched slags. According to the variation of slag structure and acid-leaching behavior, Al ions were more easily leached out by acid solution when they not only linked the chains of silicate but also replaced the Si atoms in the glassy frame. For Cu, the acid-leaching availability was roughly equal to 3 mg/L in all water quenched slags. However, the leaching concentration of Cu in air cooled slags with a higher Al mol% was elevated to about 10 mg/L.

For Cr, its acid-leaching concentrations were all below 1 mg/L in water quenched slags and the leaching concentration of A-6 was slightly higher. Fig. 8(a) shows that the leaching concentrations of Mn were ~2 mg/L in all slags. The acid-leaching behavior of Ni was similar to that of Mn. For Pb, its acid-leaching concentrations were about 1 mg/L in all slags.

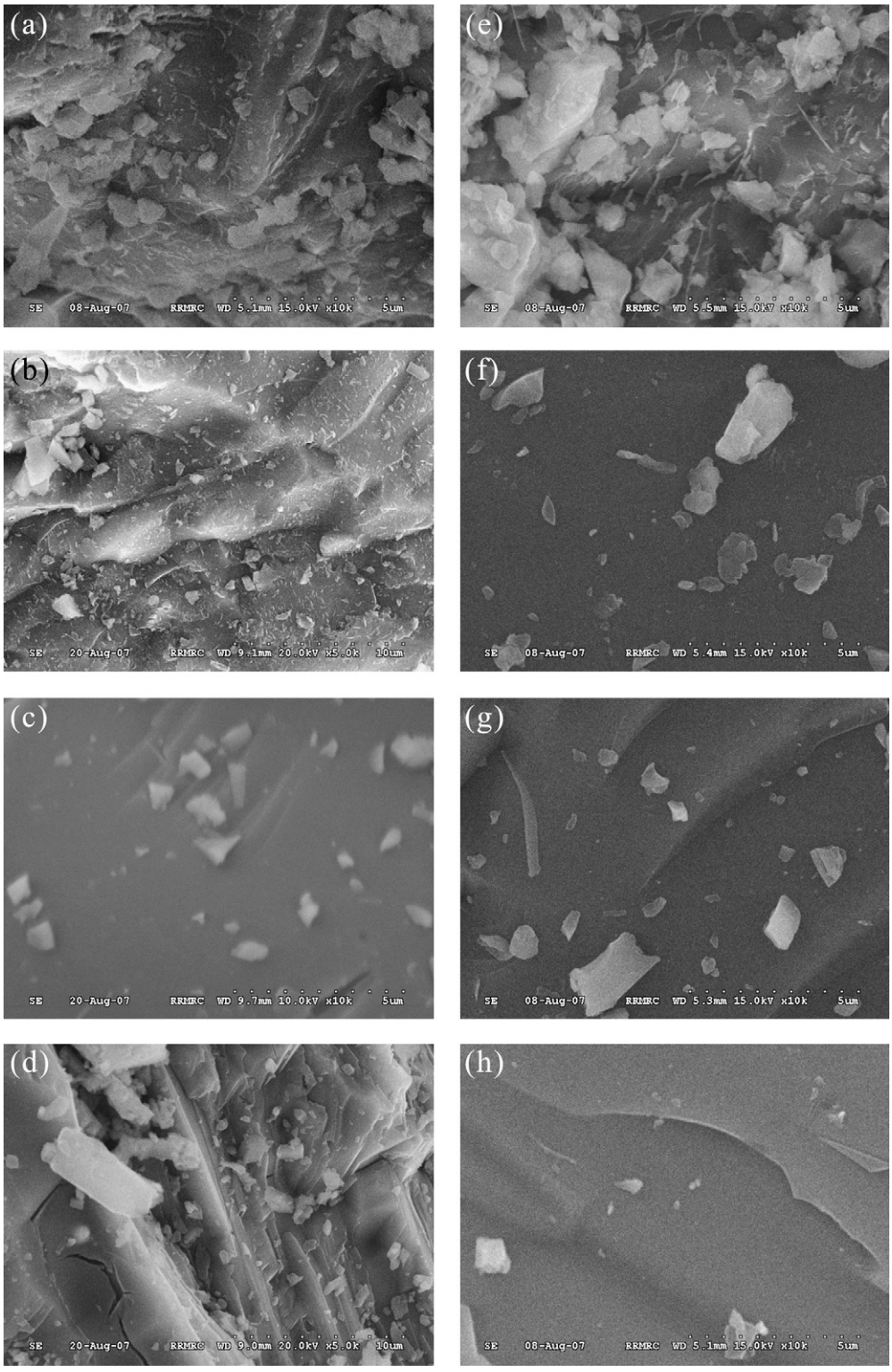

Fig. 9. SEM images of acid-immersed slags: (a) A-0, (b) A-2, (c) A-4, (d) A-6, (e) W-0, (f) W-2, (g) W-4, and (h) W-6.

Accordingly, the acid-leaching behavior of Mn, Ni, and Pb was roughly identical, and also agreed with their encapsulation behavior.

3.4. Microstructures and crystalline characteristics of acid leached slags

The SEM images of acid-immersed slags are shown in Fig. 9, and A-0/W-0, A-2/W-2, A-4/W-4, and A-6/W-6 were used to represent the acid corrosion behavior of slags. For A-0 and W-0, their crystalline structures were apparently corroded, but no sign of decomposition of amorphous glassy structure was seen. Comparing A-2 with W-2, the corrosion was significant in A-2 but this phenomenon was hardly observed in W-2. The original structures of A-4 and W-4 were both amorphous and no sign of corrosion in acid-immersed slags was observed. For A-6 and W-6, the corrosion was more significant in A-6 than in W-6, which was similar to that of A-2 and W-2. Overall, the slags with highly amorphous structures,

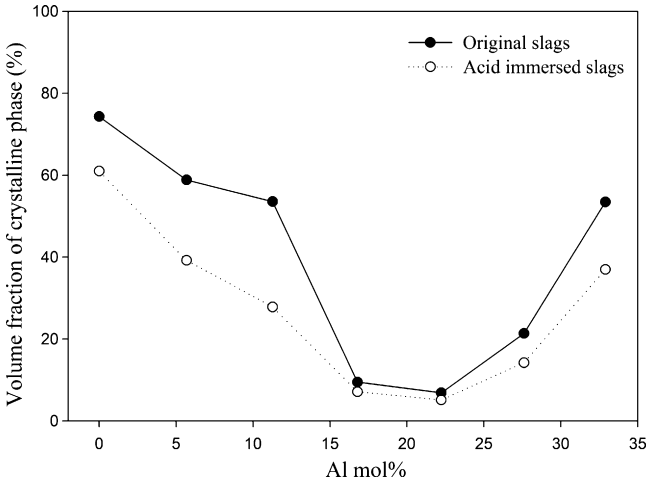

Fig. 10. Volume fractions of crystalline phase in air cooled slags.

such as A-4, W-2, W-4, and W-6, had better acid resistance, and the appearances of these slags were very similar. For slags having acicular crystalline phase ($CaSiO_3$), including A-0, W-0, and A-2, the crystalline rather than amorphous phase was drastically corroded. The SEM images of acid-immersed slags indicate that the crystalline characteristics governed the corrosion behavior of slags, and amorphous glassy slags offered better resistance to acid attacks. Similar results with regard to corrosion behavior were also reported in our previous study [20].

Fig. 10 shows the volume fraction of the crystalline phase in air cooled slags decreased after acid immersion. Moreover, when the slag had a higher volume fraction of crystalline phase, the percentage decrease was relatively higher, revealing that the amorphous phase was less attacked by acid. It is thus noted that the acid would corrode the crystalline rather than the amorphous phase in slags, and the XRD analysis results also agreed with the SEM observation.

4. Conclusions

In this study, the encapsulation of metals versus various Al mol% was evaluated by a sequential extraction procedure. According to the mobile phase distribution, Al mainly existed as the stable phase at ~5% Al mol%, while most of Al moved to the moderately mobile phase with higher Al mol%. The substitution of Al ions for Si ions reduced the immobilization of Al and also weakened the encapsulation ability of the glass matrix. Thus the immobilization of Cr was reduced, because it tended to stay in slags. However, the mobile phases of Cu, Mn, Ni, and Pb were little associated with the Al mol% or slag structure, because these metals tended to move to ingot or vaporize into flue gas. According to the results of the mobile phase distribution, water quenched slags generally offered better encapsulation of metals than air cooled slags.

The crystalline phase was easily corroded by acid, so the amorphous structure had better acid resistance, according to the SEM observation and the semi-quantitative XRD analysis. We observed that excess amount of Al_2O_3 reduced the encapsulation of metals although it is well known that Al_2O_3 may improve some slag physical properties such as hardness or tensile strength. Therefore, how to decide the optimal Al mol% in vitrification depends on the purpose of the treatment process, and deserves further investigation.

References

[1] G. Qian, Y. Cao, P. Chui, J. Tay, Utilization of MSWI fly ash for stabilization/solidification of industrial waste sludge, J. Hazard. Mater. B 129 (2006) 274–281.
[2] H.Y. Wu, Y.P. Ting, Metal extraction from municipal solid waste (MSW) incinerator fly ash—chemical leaching and fungal bioleaching, Enzyme Microb. Technol. 38 (2006) 839–847.
[3] C.R. Cheeseman, A. Makinde, S. Bethanis, Properties of lightweight aggregate produced by rapid sintering of incinerator bottom ash, Resour. Conserv. Recy. 43 (2005) 147–162.
[4] P. Chindaprasirt, C. Jaturapitakkul, T. Sinsiri, Effect of fly ash fineness on microstructure of blended cement paste, Constr. Build. Mater. 21 (2007) 1534–1541.
[5] H.J.H. Brouwers, D.C.M. Augustijn, B. Krikke, A. Honders, Use of cement and quicklime to accelerate ripening and immobilize contaminated dredging sludge, J. Hazard. Mater. 145 (2007) 8–16.
[6] G.C.C. Yang, S.Y. Chen, Statistical analysis of physicochemical properties of monoliths solidified from a municipal incinerator fly ash, J. Hazard. Mater. 45 (1996) 149–173.
[7] K. Park, J. Hyun, S. Maken, S. Jang, J.W. Park, Vitrification of municipal solid waste incinerator fly ash using Brown's gas, Energy Fuels 19 (2005) 258–262.
[8] Y.M. Kuo, T.C. Lin, P.J. Tsai, W.J. Lee, H.Y. Lin, Fate of polycyclic aromatic hydrocarbons during vitrification of incinerator ash in a coke bed furnace, Chemosphere 51 (2003) 313–319.
[9] Y.M. Kuo, T.C. Lin, P.J. Tsai, Metal behavior during vitrification of incinerator ash in a coke bed furnace, J. Hazard. Mater. B 109 (2004) 79–84.
[10] L.L. Oden, W.K. Connor, ASME/US vitrification of residue (ash) from municipal waste combustion systems, Bureau of Mines Investigation Program Report on 1994, 24, ASME Research Committee on Industrial and Municipal Wastes Subcommittee on Ash Vitrification, 1994, pp. 71–101.
[11] K. Kakimoto, Y. Nakano, T. Yamasaki, K. Shimizu, T. Idemitsu, Use of fine-grained shredder dust as a cement admixture after a melting, rapid-cooling and pulverizing process, Appl. Energy 79 (2004) 425–442.
[12] K.L. Lin, Feasibility study of using brick made from municipal solid waste incinerator fly ash slag, J. Hazard. Mater. B 137 (2006) 1810–1816.
[13] M. Kersten, U. Förstner, Speciation of trace metals in sediments and combustion waste, in: A.M. Ure, C.M. Davidson (Eds.), Chemical Speciation in the Environment, 1st ed., Chapman & Hall Glasgow, Scotland, 1995, pp. 234–275.
[14] H. Ecke, H. Sakanakura, T. Matsuto, N. Tanaka, A. Lagerkvist, Effect of electric arc vitrification of bottom ash on the mobility and fate on metals, Environ. Sci. Technol. 35 (2001) 1531–1536.
[15] B.D. Cullity, S.R. Stock, Elements of X-ray Diffraction, 3rd ed., Prentice Hall, Upper Saddle River, 2001.
[16] C.Y. Chen, G.S. Lan, W.H. Tuan, Preparation of mullite by the reaction sintering of kaolinite and alumina, J. Eur. Ceram. Soc. 20 (2000) 2519–2525.
[17] Y.M. Kuo, T.C. Lin, P.J. Tsai, Immobilization and encapsulation during vitrification of incineration ashes in a coke bed furnace, J. Hazard. Mater. B133 (2006) 75–78.
[18] W.D. Kingery, H.K. Bowen, D.R. Uhlmann, Introduction to Ceramics, 2nd ed., John Wiley & Son, Inc., New York, 1976.
[19] C.T. Li, W.J. Lee, K.L. Huang, S.F. Fu, Y.C. Lai, Vitrification of chromium electroplating sludge, Environ. Sci. Technol. 41 (2007) 2950–2956.
[20] Y.M. Kuo, J.W. Wang, H.R. Chao, C.T. Wang, G.P. Chang-Chien, Effect of cooling rate and basicity during vitrification of fly ash. Part 2. On the chemical stability and acid resistance of slags, J. Hazard. Mater. 152 (2008) 554–562.